Porphyromonas gingivalis outer membrane vesicles alter neuronal architecture and Tau phosphorylation in the embryonic mouse brain

Adrienne Bradley[1 ¶], Lauren Mashburn-Warren[1 ¶], Lexie C. Blalock[1 ¶ #a], Francesca Scarpetti[1], Christian L. Lauber[1,2*]

[1] Institute for Genomic Medicine, Nationwide Children's Hospital, Columbus, Ohio, USA

[2] Department of Pediatrics, The Ohio State University College of Medicine, Columbus, Ohio, USA

[#a] Current Address: Abbott Nutrition, Columbus, Ohio, USA

*Corresponding Author

E-mail: Christian.Lauber@nationwidechildrens.org

¶ These authors contributed equally to this work.

Abstract

Porphyromonas gingivalis (Pg) is an oral bacterial pathogen that has been associated with systemic inflammation and adverse pregnancy outcomes such as low birth weight and preterm birth. Pg drives these sequelae through virulence factors decorating the outer membrane that are present on non-replicative outer membrane vesicles (OMV) that are suspected to be transmitted systemically. Given that Pg abundance can increase during pregnancy, it is not well known whether Pg-OMV can have deleterious effects on the brain of the developing fetus. We tested this possibility by treating pregnant C57/Bl6 mice with PBS (control) and OMV from ATCC 33277 by tail vein injection every other day from gestational age 3 to 17. At gestational age 18.5, we measured dam and pup weights and collected pup brains to quantify changes in inflammation, cortical neuron density, and Tau phosphorylated at Thr231. Dam and pup weights were not altered by Pg-OMV exposure, but pup brain weight was significantly decreased in the Pg-OMV treatment group. We found a significant increase of Iba-1, indicative of microglia activation, although the overall levels of IL-1β, IL-6, TNFα, IL-4, IL-10, and TGFβ mRNA transcripts were not different between the treatment groups. Differences in IL-1β, IL-6, and TNFα concentrations by ELISA showed IL-6 was significantly lower in Pg-OMV brains. Cortical neuron density was modified by treatment with Pg-OMV as immunofluorescence showed significant decreases in Cux1 and SatB2. Overall Thr231 was increased in pups exposed to Pg-OMV with the appearance of a secondary band of 60 kD. Together these results demonstrate that Pg-OMV can significantly modify the embryonic brain and suggests that Pg may impact offspring development via multiple mechanisms.

Introduction

Pregnancy induces significant changes in mothers including shifts in the abundance of oral bacteria (1-4). Increased blood flow and pregnancy related hormones allows for the growth of pathogens like *Porphyromonas gingivalis* (Pg) an organism associated with oral infections that are increasingly linked to adverse pregnancy and neurodevelopmental outcomes (5-7). Increased Pg presence is estimated to be prevalent in 40% of pregnancies in the US and 2-11% worldwide (8, 9). This presence of bacteria sometimes resulting in periodontitis, a significant dental infection, can drive systemic inflammation (10-12). Preterm birth, preeclampsia, and low birth weight are well-characterized effects of maternal Pg infections and Pg DNA has been detected in the placenta and amnionic fluid. Pg driven outcomes affecting children have focused on pregnancy outcomes (13-18) and only recently has Pg received attention as a modulator of fetal development and remains an understudied host-pathogen interaction (19, 20).

P. gingivalis has been extensively studied to determine its role in modifying pregnancy. Rodent models of Pg infection demonstrate that exposure to Pg can result in systemic inflammation, low birth weight and pre-term delivery (21-25). Pg mediates these and other effects thorough a number of virulence factors that modify host responses including lipopolysaccharide (LPS) and proteases known as gingipains (26-32). Both are also present on the surface of OMV that are now suspected to be transmitted systemically in the blood stream (20, 32, 33). LPS and the gingipains interact with the immune system but are unique compared to other gram-negative bacteria. For instance, Pg LPS is less immunogenic than *Escherichia coli* LPS but also causes inflammation and the production

72 of pro-inflammatory cytokines (34, 35). The gingipains are unique to Pg and they modify
73 cytokine expression that allows Pg to evade the host immune response and establish
74 periodontal infections that drive systemic inflammation (36-39). Pg infection also modifies
75 the placenta to cause spiral artery remodeling that can result in a hypoxic state linked to
76 preeclampsia and fetal growth restriction (40). However, whether Pg-OMV may induce
77 fetal growth restriction—a common outcome in animal models and humans with Pg
78 infections of clinical significance—is not yet known.
79
80 *P. gingivalis* is associated with maternal inflammation and adverse pregnancy outcomes
81 that increase the risk of modified developmental trajectories of offspring (17, 41). Live Pg
82 is well demonstrated to increase inflammation in animal models and exposure to Pg-OMV
83 recapitulates these observations as the vesicles harbor the same virulence factors. Ishida
84 et al. reported increased Iba-1 indicative of microglia activation and modified
85 neuroarchitecture in E 20 pup brains from dams with an established Pg infection prior to
86 pregnancy (19). These alterations were accompanied by declines in cognitive ability, and
87 it was suggested the combined effects on the embryonic brain resulted in
88 neuroinflammation that drove these changes. Similarly, Gong et al. described a
89 neuroinflammatory phenotype in adult mice where exposure to Pg-OMV for 3 months
90 increased IL-1β and NLRP3 expression concurrent with modification of the
91 neuroarchitecture and behavior (33). Together these studies suggest that long-term
92 exposure to Pg and Pg-OMV can result in immune phenotypes indicative of a pro-
93 inflammatory response that would be expected from activated microglia in the M1
94 activation state (42, 43). However, the maternal immune system functions differently than

95 the non-pregnant state and changes in inflammation and neuroarchitecture related to
96 pathogen exposure *in utero* after pregnancy is established may also differ. This
97 knowledge gap limits our efforts to refine predictions of the potential impact of pathogen-
98 driven inflammation on the developmental trajectory of offspring.
99
100 Tau is an essential protein with multiple roles in maintaining neuron homeostasis (44-46).
101 Proper function is dependent on phosphorylation that can occur at multiple sites and can
102 be modified by inflammation and exposure to pathogens such as Pg (47-49).
103 Phosphorylated Tau (p-Tau) has less affinity for tubulins and self-aggregates into β-
104 amyloid plaques that are a hallmark of neuroinflammatory diseases such as Alzheimer's
105 and Parkinson's diseases in older adults (50). The resulting Tau tangles can trigger an
106 immune response that is sustained through microglial NFκβ signaling and thus are
107 considered pathogenic forms of the protein (51, 52). In a mouse model, Gong et al.
108 showed that Pg-OMV alter the Tau profile and could result in β-amyloid plaques
109 accompanied by increased inflammation (33). However, relatively less is known about the
110 role of p-Tau in the developing brain and whether exposure to pathogens during
111 pregnancy alters this profile. A survey of fetal and adult Tau phosphorylation in humans
112 demonstrated significant overlap in p-Tau where some of the pathogenic forms of Tau in
113 adults with Alzheimer's disease were also prevalent in the fetal brain suggesting p-Tau in
114 children does not have a pathogenic effect as observed in adults (53). Interestingly, Tau
115 is hyperphosphorylated in the embryonic rodent brain but knock-down of Tau during
116 gestation in mice can reduce neuronal migration to all cortical layers indicating that p-Tau
117 is an important part of normal brain development in mice (47, 49, 54). Whether or not Pg-

118 OMV may modulate Tau phosphorylation in developing brains *in utero* is an open
119 question. Addressing this knowledge gap may provide valuable insight into the
120 mechanisms by which Pg is able to modify developmental trajectories of children.
121
122 Herein, we describe a study to determine the effect of Pg-OMV on the developing mouse
123 brain to understand this host-pathogen interaction that frequently occurs in the human
124 population. To simulate a maternal infection with Pg, pregnant C57/Bl6 mice were
125 exposed to a consistent dose of Pg-OMV via tail vein injection. At gestational age (GA)
126 18.5, inflammatory responses, concentration of Tau Thr231 (Thr231) and neuron density
127 in the cortices of embryonic pup brains were assessed to augment the understanding of
128 Pg-modulated brain development that may be relevant to pathogen exposure during
129 pregnancy.
130

131 # Results

132 ## Pup Body and Brain Weights

133 Previous studies in mice have demonstrated that dams with Pg infection or those
134 consistently dosed with Pg bacteria during pregnancy can result in low birth weight of
135 pups. We recorded weight of the dams, pups, and pup brains at GA 18.5 (Fig 1A) to
136 determine whether exposure to Pg-OMV would have the same effect. Dam and pup
137 weights were not significantly different in PBS and Pg-OMV groups (Fig 1B and 1C) but
138 there was a significant decrease in the pup brain weight after 14 days of Pg-OMV
139 treatment (Fig 1D, Mann-Whitney U $p = 0.023$,). We included an assessment of Hif1a as
140 Pg is known to cause hypoxia in mouse models that is related to fetal growth restriction.

141 Relative expression of HiF1a in the embryonic mouse brain was not significantly different
142 between the control and treated groups indicating the OMV did not induce a hypoxic state
143 *in utero* that could account for the decreased pup brain weights (Fig 1E).
144

145 Inflammation

146 Maternal inflammation can affect the developing embryo in mouse models, and we tested
147 whether exposure to Pg-OMV during pregnancy would result in an inflammatory response
148 concordant with increased presence of pathogens experienced during pregnancy. First,
149 we assessed the concentration of Iba-1 as a surrogate of microglia activation and
150 established this immune cell typically involved in pathogen defense was active in the
151 embryonic mouse brain. Western blotting of whole brain homogenates showed that Iba-
152 1 was significantly increased in Pg-OMV pup brains compared to PBS controls (Fig 2A
153 and 2B, Mann-Whitney U $p = 0.0003$). Next, we tested whether increased Iba-1 was
154 accompanied by increased concentration and expression of pro-inflammatory cytokines
155 IL-1β, IL-6 and TNFα indicative of M1 activation that produces a pro-inflammatory
156 response. ELISA quantification showed that PBS pups typically had higher levels of
157 cytokines but only IL-6 was significantly greater in the PBS brains compared to pups from
158 the Pg-OMV group (Fig 3D, Student's T-test $p = 0.002$). The levels of IL-1β and TNFα
159 showed similar trends but were not statistically different between the treatment groups
160 (Fig 3A, 3D, 3G, $p > 0.05$ in all cases). We extended this analysis to include effects that
161 may be apparent at the level of expression in the embryonic brain tissue. RT-qPCR
162 analysis of these cytokines showed no significant difference between the PBS and Pg-
163 OMV pups. Then, we tested the possibility that increased Iba-1 could result in an M2 or

164 anti-inflammatory immune response given that microglia can be in two broad functional
165 categories (42, 55). Analysis of IL-4, IL-10 and TGFβ typical of M2 activated microglia
166 were not significantly different between the treatment groups (Fig 3 C, 3F, 3I, $p > 0.05$ in
167 all cases). Lastly, given these results we tested whether the expression of NLRP3, MyD88
168 and NFκβ, which can be modified by exposure to Pg or it's OMV, were also modified in
169 our pups. RT-qPCR analysis of MyD88 and NLRP3 transcripts (Fig 4) had similar
170 downward trends with Pg-OMV treatment but were not significantly different compared to
171 controls (Fig 4A, and 4B, $p > 0.05$ in both cases). Interestingly, NFkβ transcripts that are
172 typically reported as being upregulated by Pg were significantly decreased in the Pg-OMV
173 group (Fig 4C, Student's T-test $p = 0.004$).
174
175 We were interested in identifying potential modifications in cytokine concentration and
176 expression that may differ between female and male offspring as maternal inflammation
177 may have sex specific effects. When parsed by sex, we observed that IL-6 and IL-1β
178 concentrations were significantly lower in female pups from the Pg-OMV group compared
179 to the female controls (Fig 3A, Mann-Whitney U test $p = 0.04$ and 3D, Student's T-test p
180 $= 0.0095$) and though TNFα was lower in Pg-female pups, it was not statistically different
181 in our analysis (Fig 3A, 3D. 3G). The effect of Pg-OMV on transcription was highly variable
182 for IL-1β, TNFα, IL-4, IL-10 and TGFβ but generally trended upwards (Fig 3B-3I) for the
183 female pups. Trends in the males were similar but were not significant and likely result
184 from low sample sizes (Fig 3), though we could not assess difference in cytokine
185 concentrations as the Pg male group had only 2 observations (Fig 3A, 3D, 3G).
186

Neuroarchitecture

Without a strong inflammatory phenotype, we tested the possibility that Pg-OMV treatment could nonetheless result in differences in the neuroarchitecture of the developing mouse brain. We examined the distribution of neuronal proteins Cux1, SatB2, and Ctip2 that are differentially expressed across the layers of the cortex in sagittal sections of-embryonic mouse brains. The distribution and density of these proteins were modified by exposure to Pg-OMV compared to pups from the PBS group (Fig 5A and 5B). We saw significant decreases in Cux1 (Student's T-test $p = 0.03$) and SatB2 (Students T-test $p = 0.0001$) signal intensity but not Ctip2 (Student's T-test $p = 0.064$) although it also followed a similar downward trend in the Pg-OMV pup brains (Fig 5B). These findings suggests that cortical layering was drastically altered in Pg exposed animals.

Tau Thr231

We evaluated whether Tau phosphorylated at Thr231 in GA 18.5 mouse brains was affected by exposure to Pg-OMV during gestation as this is one form of p-Tau implicated in neuroinflammatory diseases. Western blotting of proteins from whole brain homogenates showed Thr231 was present in PBS and Pg-OMV mouse brains at approximately 50 kD indicating that at this amnio acid, Tau was in a phosphorylated state concordant with other observations of Tau in the developing mouse brain (Fig 6A). We observed that an additional band at 60kD became more prominent in the Pg-OMV brains compared to controls (Fig 6A). Quantification of these bands showed that both the 50kD and 60kD bands were significantly greater in the brains from Pg-OMV exposed mice compared to the PBS control group (Fig 6B, 50 kD Student's T-test $p = 0.003$, 60kD Student's T-test $p = 0.0006$). The increased abundance of both (e.g. 50kD signal + 60kD

211 signal = total Thr231) lead to significant overall increase of Thr231 in the Pg-OMV group
212 (Fig 6B, total Thr231, Student's T-test p = 0.001) indicating Pg-OMV may alter the total
213 concentration and diversity of Thr231 isoforms during development in our mice.
214

215 Discussion

216 Animal models of Pg infection demonstrate modified pregnancy outcomes and can alter
217 birth weight of offspring. Our experimental design did not recapitulate these observations
218 as pup weights in the Pg-OMV group were not statistically different from PBS controls.
219 Moreover, dam weights were also unchanged indicating that food and water intake were
220 likely not different between the control and treatment groups. The mechanism behind
221 reduced brain weight is not clear from our observations, although pup weight followed a
222 similar downward trend suggesting that the effect of Pg-OMV was systemic for the
223 developing embryos. It could be possible that exposure to pathogens after initiation of
224 pregnancy is different from a state where the pathogen is already present and interacting
225 with host defense mechanisms. Likewise, the dosage of Pg-OMV we used may have not
226 been sufficient to recapitulate the full effect of Pg on pregnancy outcomes, where more
227 robust responses of the host and fetus may be required to lower birth weights. This would
228 coincide with unchanged expression of Hif1a. Nevertheless, treatment with a low dosage
229 of Pg-OMV during pregnancy impacted the development of the embryonic brain that could
230 have implications after birth.
231

232 *P. gingivalis* and Pg-OMV induced neuroinflammation is suspected to be involved in
233 cognitive decline in aging cohorts and have a significant impact on development *in utero*.

234 Our hypothesis that Pg-OMV would produce a pro-inflammatory response in the
235 embryonic mouse brain was not observed. Cytokine concentrations and levels of mRNA
236 transcripts in the pup brains tended to be lower in the Pg-OMV group. The lack of
237 concordance with previous work was somewhat unexpected as most reports demonstrate
238 systemic inflammation upon exposure to Pg or its OMV. Significant increases of Iba-1 in
239 Pg-OMV exposed brains indicates sensing of bacterial-derived components, such as
240 LPS, that can stimulate immune response, though this was not accompanied by a
241 significant increase in cytokine production in our mice. Moreover, Pg has atypical LPS
242 compared to organisms like *E. coli* LPS, that can bind to TLR-4, but can be recognized
243 by alternative sensing pathways. We addressed this possibility by quantifying the
244 expression of MYD88 and NLRP3 inflammasome mRNAs that are known to increase
245 upon exposure to Pg or Pg-OMV. Our analysis found that concentrations of both were
246 unaffected by OMV treatment in GA 18.5 pup brains and we posit several factors may be
247 influencing our data. First, our results could originate from the delivery of Pg-OMV via tail
248 vein injection which bypass sensing mechanisms such as dendritic cells of the
249 gastrointestinal tract that would detect Pg and LPS being translocated from the oral cavity
250 in saliva. Second, it is equally possible that Pg-OMV induced inflammation reported
251 elsewhere may be an outcome in adult mice with long-term exposure to Pg or Pg-OMV
252 but may not necessarily be an outcome for exposure after pregnancy has been
253 established given the maternal immune system functions differently compared to the pre-
254 pregnancy state. Thus, our observations may not be comparable to reports that use Pg
255 infection or treatment with Pg or Pg-OMV at high doses over several weeks prior to
256 inducing pregnancy. Importantly, the dosing scheme described here suggests there is a

257 potential use of Pg-OMV as a proxy for bacteria to study effects on fetal tissues
258 independent of systemic inflammation driven by common oral pathogens that become
259 more prevalent during pregnancy. More work is needed to elucidate how the timing and
260 dosage of pathogen exposure relative to the start of pregnancy modulates immune
261 responses during gestation that could be associated with long-term consequences for
262 offspring in human populations.
263
264 Several reports have quantified the impact of Pg and Pg-OMV on neurons as this cell
265 type is affected by inflammation and is important in brain development. Our data indicate
266 that Pg-OMV have a significant impact on neurons as their prevalence was modified in
267 the cortical layers of the embryonic brain. Cux1, SatB2, and Ctip2 signals were lower
268 overall and showed modified distribution in the Pg-OMV exposed brains compared to
269 controls. The down regulation of SatB2 and Cux1 are particularly interesting as abnormal
270 expression of both are associated with altered behavior in mice and are suspected to be
271 a contributor to autism spectrum disorder-like symptoms in humans. Likewise,
272 deficiencies in Cux1 expression have been linked to neurodevelopmental delays, while
273 down regulation of Ctip2 is known to affect axonal growth and is involved in spiny neuron
274 differentiation. The neuroarchitectural changes observed herein are aligned with previous
275 studies, yet novel because these cortical layer aberrations were not accompanied by any
276 indication of systemic inflammation. Collectively, these data suggest that Pg, or perhaps
277 Pg-OMV specially, affect the developing brain through a different mechanism. Parsing out
278 the effects of Pg-OMV on cell proliferation and migration appears to be critical in

279 deciphering how Pg mediates effects on the developing brain and should be addressed
280 in future studies to better understand this important host-pathogen interaction.
281
282 The importance of Tau in the developing brain has not been fully described but our
283 observations indicate exposure to Pg-OMV can alter the amount of Thr231 in mouse
284 embryos. Tauopathies have multiple effects on the central nervous system including
285 sustained inflammation through NFκβ signaling microglia that detects the pathogenic form
286 of Tau in adult animal models. Our data would appear to support the notion that Thr231
287 in the embryonic mouse brain is not pathogenic as an innate immune response,
288 concordant with an inflammation-based hypothesis of neurodegenerative phenotypes,
289 was not observed. Accordingly, we did not observe an increase in NFκβ that can
290 encourage transcription of cytokines. We did not perform a comprehensive assessment
291 of Tau phosphorylation sites, nor did we specifically address potential interactions
292 between p-Tau and microglia. Nonetheless, the alteration of Thr231 abundance aids in
293 explaining how changes in neuron migration and axon growth may result from exposure
294 to Pg *in utero*; our observed changes in cortical layer markers could be the result of
295 altered microtubule binding driven by altered p-Tau. Thus, much work remains to be done
296 in elucidating the role of Pg and Pg-OMV on human neurodevelopment and cognitive
297 trajectories from the early to elderly phases of life.
298

299 # Methods

300 ## OMV Isolation

301 *Porphyromonas gingivalis* strain ATCC 33277 was grown in anaerobic conditions (85%
302 N_2, 10% CO_2, 5% H_2) using Tryptic Soy Broth (Difco cat# 211768) medium
303 supplemented with 5.0 mg ml-1 hemin (Thermo Fisher, cat# AAA1116503), 1.0 mg ml^{-1}
304 menadione (MP Biomedicals, cat # 102259), and 0.5 g L^{-1} L-cysteine-HC (MP
305 Biomedicals, cat # 101446). A cleared supernatant was produced by pelleting cells at
306 8000 rpm for 15 minutes followed by filtration of the supernatant through a 0.45 um
307 membrane filter under low vacuum pressure. Using Sorvall 11.5mL ultracentrifuge tubes
308 and ultracrimp tube plugs, filtered supernatant was ultacentrifuged at 65,000 rpm for 1
309 hour at 4°C using a Sorvall WX Ultra 80 centrifuge. Immediately after centrifugation,
310 supernatant was discarded and the pellet containing the OMV was resuspended in
311 500uL of PBS (56). The total protein of the OMV were quantified using the Pierce BCA
312 assay with BSA as a standard and stored at -20°C for future use.
313

314 Animal Breeding, Dosing and Tissue Collection

315 2-3 month old C57/Bl6 mice (male and female) were purchased from Jackson Labs
316 (Maine, USA). All animals were housed in the animal research core under 12 h light/dark
317 cycles. Mice were bred and dams were checked for plugs 2x/day. Once a plug was visible,
318 the dam was removed and was marked as gestational day 0 (GA 0). Starting at E3, 50 µg
319 Pg OMV were administered via tail vein injection every other day until GA 18.5. An equal
320 volume of sterile PBS was used for the control group. Pregnant dams were anesthetized
321 using isoflurane and pups were removed via C-sections. C Pups were decapitated and
322 whole brain and placenta were collected from each pup. Half of the pup brains were
323 randomly chosen and fixed using 4% paraformaldehyde followed by 30% sucrose prior

324 to being mounted in O.C.T. and frozen for Immunohistochemical and Immunofluorescent
325 analysis. The remaining brains were snap frozen in a liquid N_2 at time of collection and
326 used for protein, RNA, and DNA extraction. Fixed tissues were stored at 4°C and frozen
327 tissues were stored at -80°C. All experimental procedures were approved by the IACUC
328 under protocol AR21-00010.
329

330 Protein Extraction, Western Blotting and ELISA

331 Protein from snap-frozen whole brains were extracted using RIPA Buffer (cell signaling)
332 with protease inhibitor cocktail (ThermoFisher). Concentration was determined prior to
333 loading using the Pierce BCA Assay Kit (ThermoFisher) with subsequent colorimetric
334 detection using BioTek Synergy H1 microplate reader. Samples were denatured in
335 Laemmli buffer at 95°C for 5 min. 50 µg total protein from each sample was loaded onto
336 10% Mini-PROTEAN® TGX™ Precast Protein Gels (Bio-Rad) and separated for 1 h at
337 150 V. Proteins were transferred onto nitrocellulose or PVDF membranes using Turbo
338 transfer (Bio-Rad) for 7 min at 2.5 A. Membranes were incubated in Everyblot blocking
339 buffer (Bio-Rad) for 1 h at RT. For Iba-1 probe, membranes were cut at 37 kDa marker
340 and lower half was incubated with Iba1, top half was incubated with b-actin. For p-Tau,
341 membranes were cut between 75 and 100 kDa marker. Top half was incubated with
342 vinculin, bottom half was incubated with phospho-Tau (Thr231) from Cell Signaling (cat #
343 71429). All primary antibody incubations were overnight at 4°C. Membranes were washed
344 in 1X Tris-buffered saline with 0.1% Tween-20 (TBST) prior to a secondary incubation
345 with either goat anti-mouse HRP or goat anti-rabbit HRP at a dilution of 1:3000 for 1 h at
346 RT. Membranes were washed a second time with 1X TBST prior to a 5 min incubation in

347 ECL reagent (superSignal west pico plus ECL substrate kit). Blots were imaged on a Bio-
348 Rad Chemidoc. Densitometric analysis was performed in ImageLab Software (Bio-Rad).
349 Target signals were normalized to a control protein on each blot of either Vinculin or β-
350 actin. Aliquots of the RIPA extracted proteins (from above) were used to quantify the
351 cytokines by ELISA for IL-1β (Invitrogen IL-1 beta Mouse ELISA kit, cat # BMS6002), IL-
352 6 (Invitrogen IL-6 Mouse ELISA kit, cat # BMS603-2) and TNFα (Invitrogen TNF alpha
353 Mouse ELISA kit, cat # BMS607-3), from whole brains according to manufacturer's
354 protocol. All samples were run in duplicate. The average from both wells was used for
355 quantification. Original western blots can be found in Supporting information S1 and S2.
356

357 Nucleic Acid Extraction, PCR, and RT-qPCR

358 DNA and RNA was extracted for sexing embryonic mice and RT-qPCR analysis of
359 cytokine mRNAs present in the pup brains. Nucleic acids were extracted from frozen
360 whole brains using the Omega Bio-tek E.Z.N.A. kit according to manufacturer's protocol
361 (cat# R6731-01). RNA and DNA concentrations were determined using Qubit Fluorometer
362 (Applied Biosystems) prior to subsequent analysis. For sexing of pups we added 1μL DNA
363 to a reaction with the Q5 Master Mix (NEB, cat# M04925) and primer sets for amplification
364 of the IL3 (For 5'- GGG ACT CCA AGC TTC AAT CA-3', Rev 5'- TGG AGG AAG AAA AGC
365 AA-3') and Sry (For 5'-TGG GAC TGG TGA CAA TTG TC, Rev 5'-GAG TAC AGG TGT
366 GCA GCT CT-3') genes (57). PCR conditions were 95°C for 4.5 min followed by 33 cycles
367 of 95°C for 35 s, 50°C for 1 min and 72°C for 1 min. PCR products were terminated with
368 a final extension at 72°C for 5 min. Bands positive for both are labeled as male while
369 samples only expressing IL3 are labeled as female.

370

371 cDNAs for RT-qPCR were made by adding 1000 ng RNA to a reaction using the High
372 Capacity cDNA Reverse Transcription Kit (Applied Biosystems, cat# 4368814). 1μL of
373 cDNA was added per reaction with gene specific primer pair sets for GAPDH, IL-1β, IL-6,
374 TNFα, IL-4, IL-10, TGFβ, MyD88, NFκβ, and NLRP3 (Integrated DNA Technologies,
375 PrimeTime qPCR Primer Assay). All samples were run in triplicate on a QuantStudio6 Pro
376 (Applied Biosystems) using the PowerUp SYBR Green Master Mix (ThermoFisher, cat #
377 A25741). Cycling conditions are as follows: 95°C for 15s followed by 60°C for 1 min for
378 40 cycles. Gene expression was measured using the QuantStudio6 Pro detection system
379 and normalized to GAPDH. Ct values were averaged from each triplicate and used to
380 calculate the relative expression by the $2^{-(\Delta\Delta Ct)}$ method with GAPDH as the reference
381 gene.

382

383 Immunofluorescent Staining

384 Fixed brains were embedded in OCT medium and 25 μm sagittal sections were collected
385 by a cryostat. Sections were washed with PBS, blocked in PBS containing 0.1% tritonX-
386 100, and 10% donkey serum and probed with and primary antibodies to Cux1 (Protein
387 Tech 11733-1-AP; diluted 1:300), SatB2 (Abcam ab92446; diluted 1:100), and Ctip2
388 (Abcam ab-18465; diluted 1:500). Sections were then washed with PBS and incubated
389 with Alexa Fluor® secondary antibodies (Thermo Fisher Scientific) and DAPI followed by
390 mounting with Prolong Diamond Antifade (Thermo Fisher Scientific). Images were
391 acquired with an ImageXpress Micro Confocal High Content Imaging System (IXMC;
392 Molecular Devices) and analyzed using MetaXpress software (Molecular Devices).

Data Analysis

We used the analysis routines in GraphPad PRISM v. 10.0 to perform statistical analysis and plotting of data points. Outlier data points were identified by the ROUT method with Q = 1% and removed from analysis. Data were tested for normality with the Kolmogorov-Smirnov test. Group differences for data with normal distributions were tested with the two-tailed, unpaired Student's-test, otherwise statistical differences were determined with the Mann Whitney-U test. Data are presented with the median and 95% Confidence Interval (CI).

Acknowledgments

We thank Dr. Rolf Stottmann and Dr. Tracy Bedrosian in the Institute for Genomic Medicine for their guidance on collecting and analyzing the cortical neurons of the embryonic mouse brains. We also thank Dr. Juhi Bagaitkar in the Center for Microbial Pathogenesis at Nationwide Children's Hospital or her discussions on the immunological implications of *P. gingivalis* infection.

References

1. Carrillo-de-Albornoz A, Figuero E, Herrera D, Bascones-Martínez A. Gingival changes during pregnancy: II. Influence of hormonal variations on the subgingival biofilm. Journal of Clinical Periodontology. 2010;37(3):230-40.

412 2. Fujiwara N, Tsuruda K, Iwamoto Y, Kato F, Odaki T, Yamane N, et al. Significant
413 increase of oral bacteria in the early pregnancy period in Japanese women. Journal of
414 Investigative and Clinical Dentistry. 2017;8(1):e12189.
415 3. Lin W, Jiang W, Hu X, Gao L, Ai D, Pan H, et al. Ecological Shifts of
416 Supragingival Microbiota in Association with Pregnancy. Frontiers in Cellular and
417 Infection Microbiology. 2018;8.
418 4. Paropkari AD, Leblebicioglu B, Christian LM, Kumar PS. Smoking, pregnancy
419 and the subgingival microbiome. Sci Rep. 2016;6(1):30388.
420 5. Jang H, Patoine A, Wu TT, Castillo DA, Xiao J. Oral microflora and pregnancy: a
421 systematic review and meta-analysis. Sci Rep. 2021;11(1):16870.
422 6. Powell AM, Khan FZA, Ravel J, Elovitz MA. Untangling Associations of
423 Microbiomes of Pregnancy and Preterm Birth. Clinics in Perinatology. 2024;51(2):425-
424 39.
425 7. Wen P, Li H, Xu X, Zhang F, Zhao D, Yu R, et al. A prospective study on
426 maternal periodontal diseases and neonatal adverse outcomes. Acta Odontol Scand.
427 2024;83:348-55.
428 8. Kassebaum NJ, Bernabé E, Dahiya M, Bhandari B, Murray CJL, Marcenes W.
429 Global Burden of Severe Periodontitis in 1990-2010:A Systematic Review and Meta-
430 regression. Journal of Dental Research. 2014;93(11):1045-53.
431 9. Lieff S, Boggess KA, Murtha AP, Jared H, Madianos PN, Moss K, et al. The Oral
432 Conditions and Pregnancy Study: Periodontal Status of a Cohort of Pregnant Women.
433 Journal of Periodontology. 2004;75(1):116-26.

434 10. Kornman KS, Loesche WJ. The subgingival microbial flora during pregnancy. J
435 Periodontal Res. 1980;15(2):111-22.
436 11. Reyes L, Phillips P, Wolfe B, Golos TG, Walkenhorst M, Progulske-Fox A, et al.
437 Porphyromonas gingivalis and adverse pregnancy outcome. J Oral Microbiol.
438 2018;10(1):1374153.
439 12. Silva de Araujo Figueiredo C, Gonçalves Carvalho Rosalem C, Costa
440 Cantanhede AL, Abreu Fonseca Thomaz ÉB, Fontoura Nogueira da Cruz MC. Systemic
441 alterations and their oral manifestations in pregnant women. Journal of Obstetrics and
442 Gynaecology Research. 2017;43(1):16-22.
443 13. Chaparro A, Blanlot C, Ramirez V, Sanz A, Quintero A, Inostroza C, et al.
444 Porphyromonas gingivalis, Treponema denticola and toll-like receptor 2 are associated
445 with hypertensive disorders in placental tissue: a case-control study. J Periodontal Res.
446 2013;48(6):802-9.
447 14. Ercan E, Eratalay K, Deren O, Gur D, Ozyuncu O, Altun B, et al. Evaluation of
448 periodontal pathogens in amniotic fluid and the role of periodontal disease in pre-term
449 birth and low birth weight. Acta Odontol Scand. 2013;71(3-4):553-9.
450 15. Gonzales-Marin C, Spratt DA, Millar MR, Simmonds M, Kempley ST, Allaker RP.
451 Levels of periodontal pathogens in neonatal gastric aspirates and possible maternal
452 sites of origin. Mol Oral Microbiol. 2011;26(5):277-90.
453 16. Katz J, Chegini N, Shiverick KT, Lamont RJ. Localization of P. gingivalis in
454 preterm delivery placenta. J Dent Res. 2009;88(6):575-8.

455 17. Leon R, Silva N, Ovalle A, Chaparro A, Ahumada A, Gajardo M, et al. Detection
456 of Porphyromonas gingivalis in the amniotic fluid in pregnant women with a diagnosis of
457 threatened premature labor. J Periodontol. 2007;78(7):1249-55.
458 18. Swati P, Ambika Devi K, Thomas B, Vahab SA, Kapaettu S, Kushtagi P.
459 Simultaneous detection of periodontal pathogens in subgingival plaque and placenta of
460 women with hypertension in pregnancy. Arch Gynecol Obstet. 2012;285(3):613-9.
461 19. Ishida E, Furusho H, Renn T-Y, Shiba F, Chang H-M, Oue H, et al. Mouse
462 maternal odontogenic infection with Porphyromonas gingivalis induces cognitive decline
463 in offspring. Frontiers in Pediatrics. 2023;11.
464 20. Lara B, Loureiro I, Gliosca L, Castagnola L, Merech F, Gallino L, et al.
465 Porphyromonas gingivalis outer membrane vesicles shape trophoblast cell metabolism
466 impairing functions associated to adverse pregnancy outcome. Journal of Cellular
467 Physiology. 2023;238(11):2679-91.
468 21. Ao M, Miyauchi M, Furusho H, Inubushi T, Kitagawa M, Nagasaki A, et al. Dental
469 Infection of Porphyromonas gingivalis Induces Preterm Birth in Mice. PLOS ONE.
470 2015;10(8):e0137249.
471 22. Konishi H, Urabe S, Miyoshi H, Teraoka Y, Maki T, Furusho H, et al. Fetal
472 Membrane Inflammation Induces Preterm Birth Via Toll-Like Receptor 2 in Mice With
473 Chronic Gingivitis. Reprod Sci. 2019;26(7):869-78.
474 23. Konishi H, Urabe S, Teraoka Y, Morishita Y, Koh I, Sugimoto J, et al.
475 Porphyromonas gingivalis, a cause of preterm birth in mice, induces an inflammatory
476 response in human amnion mesenchymal cells but not epithelial cells. Placenta.
477 2020;99:21-6.

478 24. Lin D, Smith MA, Champagne C, Elter J, Beck J, Offenbacher S. Porphyromonas
479 gingivalis infection during pregnancy increases maternal tumor necrosis factor alpha,
480 suppresses maternal interleukin-10, and enhances fetal growth restriction and
481 resorption in mice. Infect Immun. 2003;71(9):5156-62.
482 25. Yoshida S, Hatasa M, Ohsugi Y, Tsuchiya Y, Liu A, Niimi H, et al.
483 Porphyromonas gingivalis Administration Induces Gestational Obesity, Alters Gene
484 Expression in the Liver and Brown Adipose Tissue in Pregnant Mice, and Causes
485 Underweight in Fetuses. Frontiers in Cellular and Infection Microbiology. 2022;11.
486 26. Choi J-W, Kim S-C, Hong S-H, Lee H-J. Secretable Small RNAs via Outer
487 Membrane Vesicles in Periodontal Pathogens. Journal of Dental Research.
488 2017;96(4):458-66.
489 27. Gui MJ, Dashper SG, Slakeski N, Chen Y-Y, Reynolds EC. Spheres of influence:
490 Porphyromonas gingivalis outer membrane vesicles. Molecular Oral Microbiology.
491 2016;31(5):365-78.
492 28. Ho M-H, Chen C-H, Goodwin JS, Wang B-Y, Xie H. Functional Advantages of
493 Porphyromonas gingivalis Vesicles. PLOS ONE. 2015;10(4):e0123448.
494 29. Okamura H, Hirota K, Yoshida K, Weng Y, He Y, Shiotsu N, et al. Outer
495 membrane vesicles of Porphyromonas gingivalis: Novel communication tool and
496 strategy. Japanese Dental Science Review. 2021;57:138-46.
497 30. Veith PD, Chen Y-Y, Gorasia DG, Chen D, Glew MD, O'Brien-Simpson NM, et al.
498 Porphyromonas gingivalis Outer Membrane Vesicles Exclusively Contain Outer
499 Membrane and Periplasmic Proteins and Carry a Cargo Enriched with Virulence
500 Factors. Journal of Proteome Research. 2014;13(5):2420-32.

501 31. Zhang J, Yu C, Zhang X, Chen H, Dong J, Lu W, et al. Porphyromonas gingivalis
502 lipopolysaccharide induces cognitive dysfunction, mediated by neuronal inflammation
503 via activation of the TLR4 signaling pathway in C57BL/6 mice. J Neuroinflammation.
504 2018;15(1):37.
505 32. Nara PL, Sindelar D, Penn MS, Potempa J, Griffin WST. Porphyromonas
506 gingivalis Outer Membrane Vesicles as the Major Driver of and Explanation for
507 Neuropathogenesis, the Cholinergic Hypothesis, Iron Dyshomeostasis, and Salivary
508 Lactoferrin in Alzheimer's Disease. J Alzheimers Dis. 2021;82(4):1417-50.
509 33. Gong T, Chen Q, Mao H, Zhang Y, Ren H, Xu M, et al. Outer membrane vesicles
510 of Porphyromonas gingivalis trigger NLRP3 inflammasome and induce
511 neuroinflammation, tau phosphorylation, and memory dysfunction in mice. Front Cell
512 Infect Microbiol. 2022;12:925435.
513 34. Lan C, Chen S, Jiang S, Lei H, Cai Z, Huang X. Different expression patterns of
514 inflammatory cytokines induced by lipopolysaccharides from Escherichia coli or
515 Porphyromonas gingivalis in human dental pulp stem cells. BMC Oral Health.
516 2022;22(1):121.
517 35. Qiu C, Yuan Z, He Z, Chen H, Liao Y, Li S, et al. Lipopolysaccharide Preparation
518 Derived From Porphyromonas gingivalis Induces a Weaker Immuno-Inflammatory
519 Response in BV-2 Microglial Cells Than Escherichia coli by Differentially Activating
520 TLR2/4-Mediated NF-κB/STAT3 Signaling Pathways. Frontiers in Cellular and Infection
521 Microbiology. 2021;11.

522 36. Bodet C, Chandad F, Grenier D. Modulation of cytokine production by
523 Porphyromonas gingivalis in a macrophage and epithelial cell co-culture model.
524 Microbes and Infection. 2005;7(3):448-56.
525 37. Castillo Y, Castellanos JE, Lafaurie GI, Castillo DM. Porphyromonas gingivalis
526 outer membrane vesicles modulate cytokine and chemokine production by gingipain-
527 dependent mechanisms in human macrophages. Archives of Oral Biology.
528 2022;140:105453.
529 38. Charoensaensuk V, Chen YC, Lin YH, Ou KL, Yang LY, Lu DY. Porphyromonas
530 gingivalis Induces Proinflammatory Cytokine Expression Leading to Apoptotic Death
531 through the Oxidative Stress/NF-κB Pathway in Brain Endothelial Cells. Cells.
532 2021;10(11).
533 39. Palm E, Khalaf H, Bengtsson T. Porphyromonas gingivalis downregulates the
534 immune response of fibroblasts. BMC Microbiology. 2013;13(1):155.
535 40. Yang K, Xu S, Zhao H, Liu L, Lv X, Hu F, et al. Hypoxia and Porphyromonas
536 gingivalis-lipopolysaccharide synergistically induce NLRP3 inflammasome activation in
537 human gingival fibroblasts. International Immunopharmacology. 2021;94:107456.
538 41. Offenbacher S, Katz V, Fertik G, Collins J, Boyd D, Maynor G, et al. Periodontal
539 infection as a possible risk factor for preterm low birth weight. J Periodontol. 1996;67(10
540 Suppl):1103-13.
541 42. Zhang B, Wei YZ, Wang GQ, Li DD, Shi JS, Zhang F. Targeting MAPK Pathways
542 by Naringenin Modulates Microglia M1/M2 Polarization in Lipopolysaccharide-
543 Stimulated Cultures. Front Cell Neurosci. 2018;12:531.

544 43. Frank-Cannon TC, Alto LT, McAlpine FE, Tansey MG. Does neuroinflammation
545 fan the flame in neurodegenerative diseases? Mol Neurodegener. 2009;4:47.
546 44. Gao Y, Tan L, Yu JT, Tan L. Tau in Alzheimer's Disease: Mechanisms and
547 Therapeutic Strategies. Curr Alzheimer Res. 2018;15(3):283-300.
548 45. Morris SL, Brady ST. Tau phosphorylation and PAD exposure in regulation of
549 axonal growth. Frontiers in Cell and Developmental Biology. 2023;10.
550 46. Seubert P, Mawal-Dewan M, Barbour R, Jakes R, Goedert M, Johnson GV, et al.
551 Detection of phosphorylated Ser262 in fetal tau, adult tau, and paired helical filament
552 tau. J Biol Chem. 1995;270(32):18917-22.
553 47. Brion J-P, Smith C, Couck A-M, Gallo J-M, Anderton BH. Developmental
554 Changes in τ Phosphorylation: Fetal τ Is Transiently Phosphorylated in a Manner Similar
555 to Paired Helical Filament-τ Characteristic of Alzheimer's Disease. Journal of
556 Neurochemistry. 1993;61(6):2071-80.
557 48. Tang Z, Liang D, Cheng M, Su X, Liu R, Zhang Y, et al. Effects of
558 Porphyromonas gingivalis and Its Underlying Mechanisms on Alzheimer-Like Tau
559 Hyperphosphorylation in Sprague-Dawley Rats. Journal of Molecular Neuroscience.
560 2021;71(1):89-100.
561 49. Yu Y, Run X, Liang Z, Li Y, Liu F, Liu Y, et al. Developmental regulation of tau
562 phosphorylation, tau kinases, and tau phosphatases. J Neurochem. 2009;108(6):1480-
563 94.
564 50. Arendt T, Stieler JT, Holzer M. Tau and tauopathies. Brain Res Bull. 2016;126(Pt
565 3):238-92.

566 51. Wang C, Fan L, Khawaja RR, Liu B, Zhan L, Kodama L, et al. Microglial NF-κB
567 drives tau spreading and toxicity in a mouse model of tauopathy. Nature
568 Communications 2015 6. 2022;13(1):1969.
569 52. Perea JR, Ávila J, Bolós M. Dephosphorylated rather than hyperphosphorylated
570 Tau triggers a pro-inflammatory profile in microglia through the p38 MAPK pathway.
571 Experimental Neurology. 2018;310:14-21.
572 53. Hefti MM, Kim S, Bell AJ, Betters RK, Fiock KL, Iida MA, et al. Tau
573 Phosphorylation and Aggregation in the Developing Human Brain. J Neuropathol Exp
574 Neurol. 2019;78(10):930-8.
575 54. Sapir T, Frotscher M, Levy T, Mandelkow EM, Reiner O. Tau's role in the
576 developing brain: implications for intellectual disability. Hum Mol Genet.
577 2012;21(8):1681-92.
578 55. Mishra A, Bandopadhyay R, Singh PK, Mishra PS, Sharma N, Khurana N.
579 Neuroinflammation in neurological disorders: pharmacotherapeutic targets from bench
580 to bedside. Metab Brain Dis. 2021;36(7):1591-626.
581 56. Mashburn LM, Whiteley M. Membrane vesicles traffic signals and facilitate group
582 activities in a prokaryote. Nature. 2005;437(7057):422-5.
583 57. Lambert J-F, Benoit BO, Colvin GA, Carlson J, Delville Y, Quesenberry PJ. Quick
584 sex determination of mouse fetuses. Journal of Neuroscience Methods. 2000;95(2):127-
585 32.
586
587
588
589

Figures

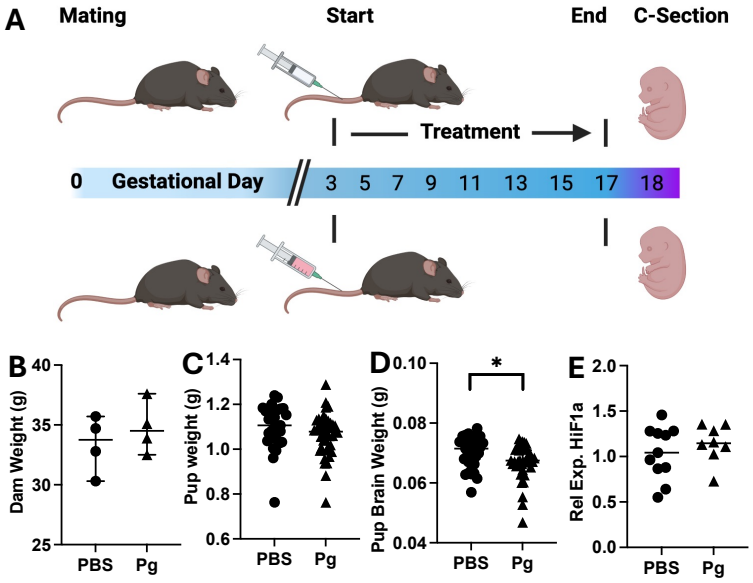

Fig 1. Experimental design and pup body and brain weights.

(A) C57/Bl6 mice were mated for up to 3 days until the appearance of vaginal plugs. The first observation of a plug was considered GA 0. Female mice were separated from the males and treated with PBS or 50 ug Pg-OMV every other day from GA 3 to GA17. Dams were sacrificed on GA 18.5 and pups delivered by C-Section for tissue collection. (B) and (C) Weight of dams and pups were not significantly different from PBS controls. (D) Brain weight decreased significantly with Pg exposure (Mann-Whitney U $p = 0.023$). (E) Relative expression of Hif1a as indicator of hypoxia in the pup brain. Relative expression calculated by the $2^{-(\Delta\Delta Ct)}$ method with GAPDH as the reference gene. Data are shown as median with 95% CI.

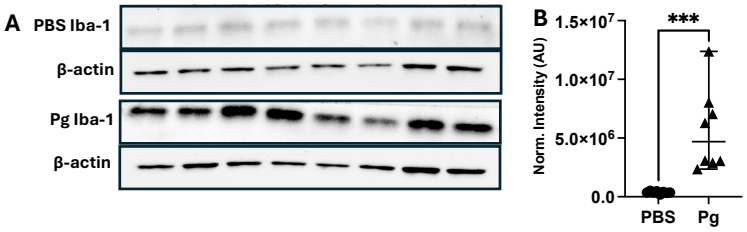

Fig 2. Increased Iba-1 in mouse pups exposed to Pg-OMV during pregnancy. **(A)** Western blot of Iba-1 and β-actin in GA 18.5 pups from PBS and Pg-OMV exposed dams. Full blot can be found in the Supporting information. **(B)** Comparison of band β-actin normalized signal intensity of Iba-1 showed significant increase in Iba-1 in the Pg-OMV group compared to controls (Mann-Whitney U p = 0.0003). Data are shown as median with 95% CI.

634

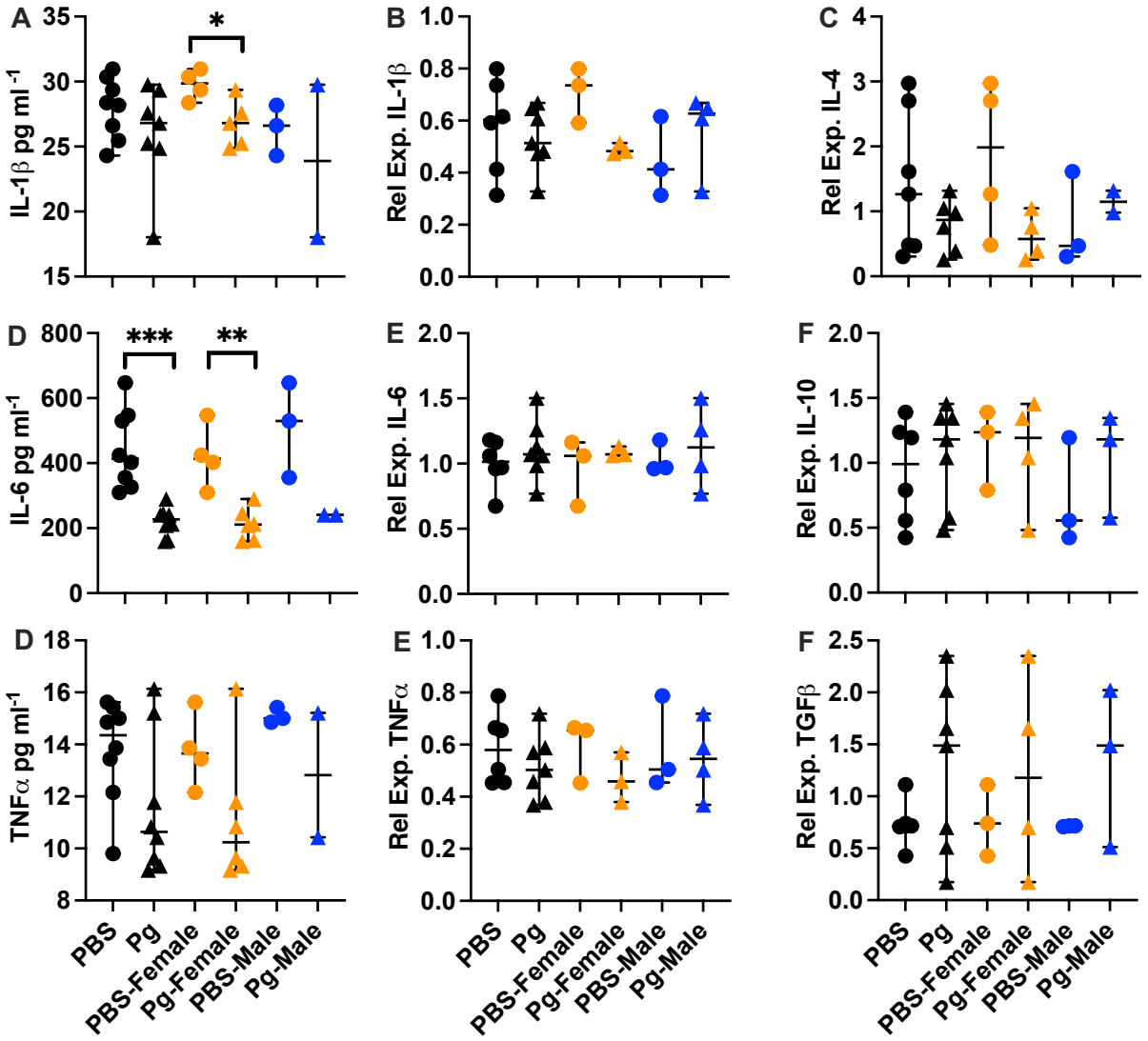

635

636 **Fig 3. ELISA and RT-qPCR evaluation of cytokines in the embryonic mouse brain.**

637 **(A, D, G)**: ELISA of IL-1β, IL-6, and TNFα in pg ml^{-1}. Cytokines were extracted from frozen

638 whole brains and quantified. IL-1β was significantly greater in the PBS female pups

639 compared to the female pups from the Pg-OMV group (Fig 3A, Mann-Whitney U test p =

640 0.04). IL-6 was significantly greater in the PBS group and in the female pups compared

641 to the OMV treatment group (Fig 3D, Student's T-test p = 0.002 and 0.0095, respectively.)

642 **(B, E, H)**: RT-qPCR of proinflammatory cytokines IL-1β, IL-6, and TNFα. **(C, F, I)**: RT-
643 qPCR of anti-inflammatory cytokines IL-4, IL-10, and TGFβ. Total RNA was extracted from
644 frozen whole brains and reverse transcribed to cDNA. Relative expression calculated by
645 the $2^{-(\Delta\Delta Ct)}$ method with GAPDH as the reference gene. Group differences for the ELISAs
646 on the males was not determined due to low sample size (n = 2). Only significant
647 differences are shown. Data are presented with the median and 95% CI. Symbols: Circles
648 = PBS, triangles = Pg; orange = females; blue = males.
649
650
651
652
653
654
655
656
657
658
659
660
661
662
663
664

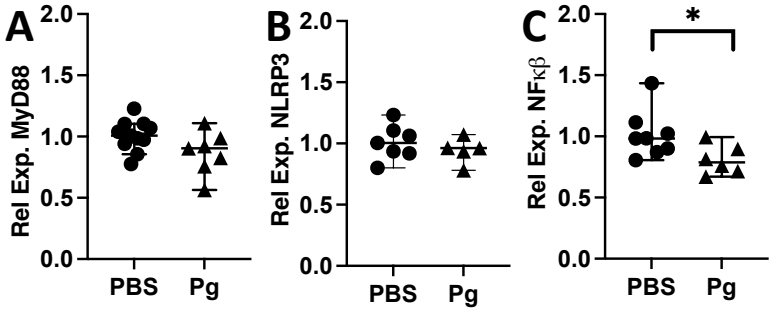

Fig 4. RT-qPCR evaluation of MYD88, NLRP3, and NFκβ in GA 18.5 pup brains. (A) MYD88 and **(B)** NLRP3 were not significantly different in pup brains from the control or treatment group. **(C)** NFkβ was significantly reduced in the pup brains (Student's T-test p = 0.004). Total RNA was extracted from frozen whole brains and reverse transcribed to cDNA. Relative expression calculated by the $2^{-(\Delta\Delta Ct)}$ method with GAPDH as the reference gene. Means across fore, mid, and hind brain sections are shown for each sample. Data are presented with the median value and 95% CI.

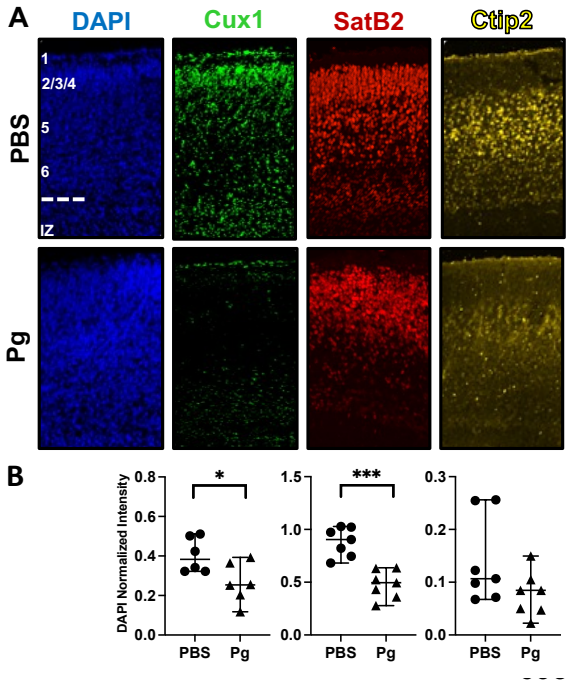

694

695 **Fig 5. Modified intensity and location of cortical layer marker proteins following Pg-**
696 **OMV exposure *in utero*. (A)** Representative immunofluorescent images from sagittal
697 sections of PFA fixed brains at GA 18.5 pup brains showing location of cortical layer
698 markers Cux1, SatB2, and Ctip2. Approximate position of cortical layers 1-6 with the
699 intraventricular zone (IZ) are shown in the PBS-DAPI image. **(B)** Quantification and
700 comparison of cortical layer proteins stained with the marker antibodies. Intensities were
701 averaged across three serial section per sample for statistical analysis. Cux1 (Student's
702 T-test p = 0.03) and SatB2 (students T-test p = 0.0001) were significantly reduced in the
703 Pg-OMV group. Data are presented with the median and 95% CI.

704

705

706

707

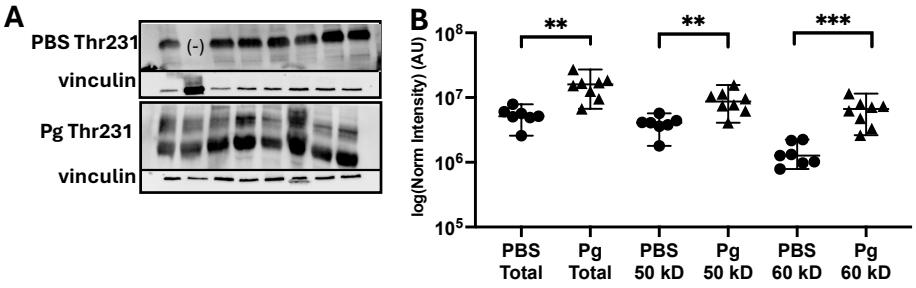

Fig 6. Thr231 is elevated in the embryonic mouse brain after exposure to Pg-OMV. **(A)** Images of Thr231 western blots. 20 ug of total protein extracted from whole, frozen GA 18.5 pup brains were analyzed. A band of approximately 60 kD became more prominent in the brains of all pups exposed to Pg-OMV during pregnancy. **(B)** Densitometry analysis of Thr231 abundance by western blot normalized to vinculin. Total Thr231 was estimated by summing the vinculin normalized intensity of the 50 kD + 60 kD bands. Total Thr231 (Student's T-test p = 0.001), 50kD (Student's T-test p = 0.003) and 60kD Thr231 quantities (Student's T-test p = 0.0006) were significantly greater in the Pg-OMV brains. Data are presented with the median and 95% CI.

Supporting Information

S1. Iba-1 and Thr231 western blots.